Antiviral Research 168 (2019) 82–90

Contents lists available at ScienceDirect

Antiviral Research

journal homepage: www.elsevier.com/locate/antiviral

Development of a rapid antiviral screening assay based on eGFP reporter virus of Mayaro virus

Xiaodan Li[a,b], Hongqing Zhang[a], Yanan Zhang[a], Jiaqi Li[a], Zhen Wang[a], Chenglin Deng[a], Ana Carolina Gomes Jardim[c], Ana Carolina B. Terzian[d], Maurício Lacerda Nogueira[d], Bo Zhang[a,*]

[a] Key Laboratory of Special Pathogens and Biosafety, Wuhan Institute of Virology, Chinese Academy of Sciences, Wuhan, 430071, China
[b] Hunan Normal University School of Medicine, Changsha, 410081, China
[c] Laboratory of Virology, Institute of Biomedical Sciences, Federal University of Uberlândia, Brazil
[d] São José do Rio Preto School of Medicine (FAMERP), São José do Rio Preto, SP, Brazil

ARTICLE INFO

Keywords:
Mayaro virus
Reverse genetics
Reporter virus
Antiviral drug discovery

ABSTRACT

Mayaro virus (MAYV) is a neglected mosquito-borne alphavirus that causes illness similar to Chikungunya (CHIKV), Dengue (DENV) and Zika virus (ZIKV). Currently, there is no specific treatment or vaccine against MAYV infection. To develop an efficient antiviral screening assay for MAYV, we constructed the infectious clones of MAYV strain BeAr 20290 and its eGFP reporter virus. The reporter virus exhibited high replication capacity indistinguishable with the wild type MAYV, and was genetically stable within at least five rounds of passages in BHK-21 cell. The expression of eGFP correlated well with the viral replication. Using the known inhibitor ribavirin, we confirmed that the MAYV-eGFP reporter virus could be used for antiviral screening to identify the specific inhibitors against MAYV. Using the MAYV-eGFP based antiviral assay, we found that the compound 6-Azauridine which had antiviral activity against CHIKV and SFV, showed a significant inhibitory effect on MAYV replication.

1. Introduction

Mayaro virus belongs to the Alphavirus genus of the Togaviridae which consists of many important human pathogenic viruses such as Chikungunya virus (CHIKV), Ross River virus (RRV), Sindbis virus (SINV) and Venezuelan equine encephalitis virus (VEEV) (Strauss and Strauss, 1994). The MAYV genome is a single-stranded positive sense RNA and composed of two open reading frames (ORF) flanked by untranslated regions (UTR) with a 5′ cap and a 3′ ploy-A tail. The 5′ ORF encodes a polyprotein from which four nonstructural proteins (nsP1-4) that are required for virus replication and pathogenesis, are formed by proteolytic cleavage. The 3′ ORF is translated from a subgenomic messenger RNA which is transcribed from the 3' one-third of the genome, and encodes a polyprotein which is processed into five structural proteins (Capsid, E3, E2, 6K and E1) that are involved in viral particle formation (Firth et al., 2008).

Since its first isolation from the blood of five febrile patients in Mayaro country, Trinidad in 1954 (Anderson et al., 1957), MAYV has been reported as causing sporadic outbreaks in tropical regions of South American countries including Brazil, Bolivia, Peru, French Guiana and Venezuela (Acosta-Ampudia et al., 2018). Recently, several imported cases have been reported in North America (Taylor et al., 2005) and European regions (Friedrich-Janicke et al., 2014; Neumayr et al., 2012). MAYV is an arthropod-borne virus that is mainly transmitted by *Haemagogus* mosquitoes, the same vector responsible for YFV transmission living in forests, with a sylvatic cycle involving non-human primates and mosquitoes (Mourao et al., 2012). Occasionally, the virus can be transmitted from non-human primates to human when they are in close proximity to the forest (LeDuc et al., 1981). Besides, MAYV has been detected in several other vertebrate hosts such as rodents and birds which presumably increase the likelihood that the virus will spread to other areas (de Thoisy et al., 2003). In addition, the *Aedes aegypti* mosquito which is responsible for the transmission of CHIKV and Zika virus, has been shown to transmit MAYV in the experimental test (Long et al., 2011). In 2015, an 8-year-old child from Haiti was diagnosed with co-infection for MAYV and dengue virus, further suggesting that *Aedes aegypti* might be involved in viral transmission (Lednicky et al., 2016). Due to the similar vectors, MAYV becomes a potential emerging arbovirus with rapid expansion in urban areas as observed for CHIKV and ZIKV previously.

The symptoms caused by MAYV infection include acute fever, rash, headache, myalgia and arthralgia/arthritis, and > 50% of the infection

* Corresponding author.
E-mail address: zhangbo@wh.iov.cn (B. Zhang).

https://doi.org/10.1016/j.antiviral.2019.05.013
Received 12 March 2019; Received in revised form 26 May 2019; Accepted 28 May 2019
Available online 29 May 2019

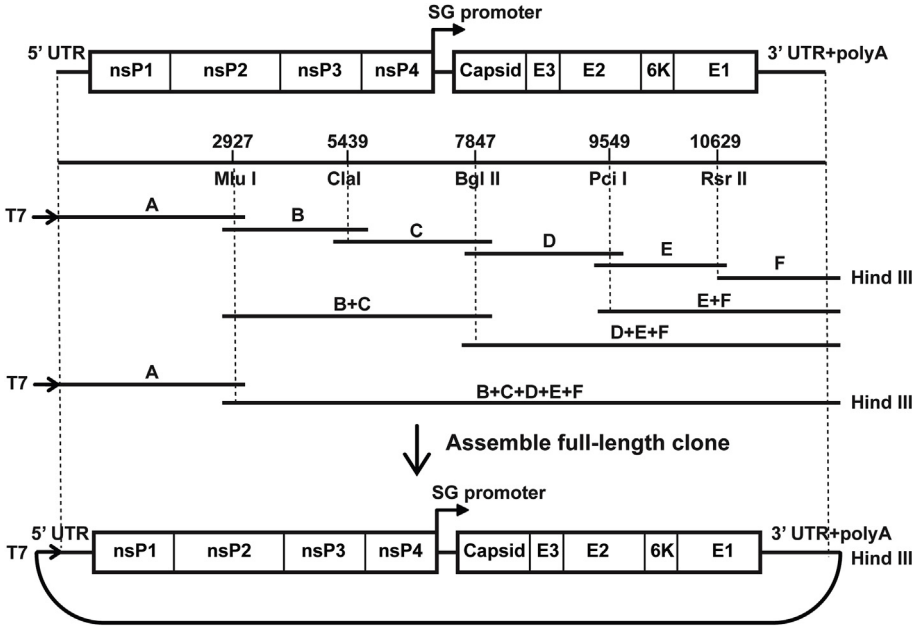

Fig. 1. Scheme of the strategy to construct the MAYV infectious clone. Genome organization and the positions of restriction sites used for assembly the full-length infectious clone are shown at the top. Six cDNA fragments (A–F) covering the complete MAYV genome were commercially synthesized. A T7 promoter was fused upstream of the 5′UTR in fragment A, and a poly-A tail was added downstream of the 3′UTR in fragment F. Individual fragments were assembled to form the full-length cDNA clone (pACYC-MAYV) by stepwise cloning using the depicted restriction sites.

cases suffer the severe and prolonged arthralgia which may last for months or years (Acosta-Ampudia et al., 2018). Most of the symptoms are in common with those of CHIKV, DENV and ZIKV infections, leading to a high chance of misdiagnosis of MAYV infection cases (Brunini et al., 2017). Together with the insufficient surveillance and lack of the diagnostic capacity in the endemic area, MAYV infections are likely underreported and widely neglected. Until now, there are no specific treatments and licensed vaccines against MAYV infection; therefore, it is necessary to develop antiviral agents and vaccines to control the virus infection and expansion.

Currently, the cell-based antiviral assay relying on viral infection of susceptible cells has been employed in MAYV drug discovery (Amorim et al., 2017; Caldas et al., 2018; Camini et al., 2018; Carvalho et al., 2014). The antiviral activity is evaluated through viral titer determination and viral RNA quantification. So far, a few compounds derived from natural products have been identified to have antiviral activity against MAYV through these approaches (Amorim et al., 2017; Caldas et al., 2018; Camini et al., 2018). However, these methods involve of multiple steps which are time-consuming, preventing them being used in high-throughput screening of large compound libraries. Thus, development of a sensitive and efficient assay system for HTS is crucial for screening potent candidates against MAYV.

Reporter virus, which is generated by inserting specific reporter gene into the viral genome, is able to real-time monitor viral replication and spread in the infected cells and animals. It has been a powerful tool for HTS for antiviral studies of many viruses such as flaviviruses (Zou et al., 2011), enteroviruses (Shang et al., 2013; Zhang et al., 2017) and influenza viruses (Weisshaar et al., 2016). For alphaviruses, reporter viruses have been reported for CHIKV (Henrik Gad et al., 2012; Kummerer et al., 2012; Vanlandingham et al., 2005), RRV (Ralambondrainy et al., 2018), SINV (Pierro et al., 2003; Sun et al., 2014), VEEV (Phillips et al., 2016) and Semliki Forest virus (SFV) (Tamberg et al., 2007) by three strategies basically. One of them is that the reporter genes insert into nsP3 gene to form nsP3-fusion proteins. However, nsP3-eGFP fused SFV is genetically unstable after two rounds of passages (Tamberg et al., 2007). Another strategy is that reporter genes insert into the genome between nsP3 and nsP4 flanked by duplications of nsP3/4 nsP2 protease-recognition site. Using this strategy, the eGFP reporter SFV showed good stability after five rounds of passages, but the viral replication was delayed compared to parental virus (Tamberg et al., 2007). In addition, several reporter alphaviruses had been established by introducing an additional subgenomic promoter to express the reporter genes. In our previous study, we had constructed a CHIKV-eGFP reporter virus with dual sg promoter and identified that the reporter gene could be stably maintained after five rounds of passages (Deng et al., 2016).

Here, we developed and characterized a stable eGFP reporter virus for the strain BeAr 20290 of MAYV which is isolated from *Haemagogus* mosquitoes in Brazil and widely used as a prototype for MAYV infection (Esposito and da Fonseca, 2015). The MAYV-eGFP replicated efficiently with similar properties to the parental MAYV and was genetically stable after at least five rounds of passages. The eGFP expression level could reflect viral replication well. Using the known inhibitors of alphavirus, we showed that MAYV-eGFP could be a powerful tool for antiviral screening.

2. Materials and methods

2.1. Cells, viruses and antibodies

Baby hamster kidney cell (BHK-21) was propagated in Dulbecco's modified Eagle's medium (DMEM) supplemented with 10% fetal bovine serum (FBS), 100 units/mL of penicillin and 100 μg/mL of streptomycin. The mosquito cell C6/36 was grown in RPMI 1640 medium supplemented with 10% fetal bovine serum (FBS), 100 units/mL of penicillin and 100 μg/mL of streptomycin. The BHK-21 and C6/36 cells were maintained in 5% CO_2 at 37 °C and 28 °C respectively. The parental MAYV and MAYV-eGFP were produced by transfection of BHK-21 cells with *in vitro* transcribed RNAs from the MAYV and MAYV-eGFP infectious clones (described below) respectively. The mouse polyclonal antibody against MAYV E2 was generated by immunization of BALB/C mice with SDS-PAGE purified MAYV E2 protein. FITC-conjugated goat anti-mouse IgG used as secondary antibody was purchased from Protein Tech Group Inc.

2.2. Plasmid construction

The overall scheme of the cloning strategy for construction of the full-length infectious clone of MAYV strain BeAr 20290 (GenBank accession no. KT754168) was shown in Fig. 1. Briefly, six cDNA fragments (designated as fragment A-F respectively) covering the full-length genome of MAYV were artificially synthesized by the DNA synthesis

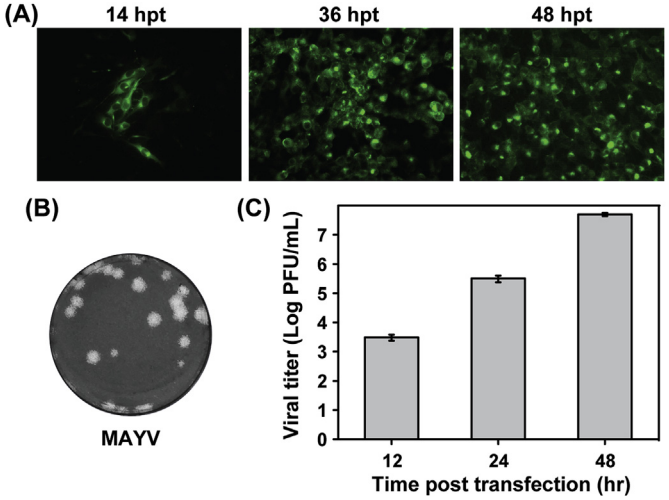

Fig. 2. Characterization of the recombinant virus. (A) IFA of viral protein expression in BHK-21 cells transfected with the MAYV RNA transcribed from the linearized pACYC-MAYV. IFA was performed at the indicated time points post transfection using the antibody against the E2 protein. (B) Plaque morphology of the recombinant MAYV. (C) Viral yield of recombinant MAYV after transfection. The supernatants from the transfected cells were collected at the indicated time points after transfection and viral titers were determined by plaque assay in BHK-21 cells. Error bars indicate the standard deviations from three independent experiments.

company TSINGKE (China). Fragment A contained a T7 promoter proceeding the sequence from the 5′UTR to 2965 nt of the genome; fragment B, C, D and E contained the sequences from nucleotide position 2857 to 5477 nt, 5335 to 7871 nt, 7809 to 9581 nt and 9520 to 10695 nt of the genome respectively. Fragment F included the sequences from 10621 nt to 3′UTR of the genome with a poly-A tail. Fragment A, D, E and F were cloned into low-copy-number vector pACYC177 at the *Bam*H I and *Hind* III sites respectively, whereas fragment B and C were inserted into pUC19 at the sites of *Bam*H I and *Hind* III. Next, fragment B + C was generated by engineering fragment C into fragment B at the *Cla* I and *Hind* III sites; meanwhile, fragment E + F was constructed by *Rsr* II and *Hind* III digestion, and then fragment D was inserted into fragment E + F at *BamH* I and *Pci* I sites generating fragment D-F. After that, fragment B-F was constructed by pasting fragment B + C into fragment D-F at the *Mlu* I and *Hind* III sites. At last, the infectious clone pACYC-MAYV which contained a T7 promoter and complete genome of MAYV BeAr 20290 strain was obtained by assembly fragment A into fragment B-F at *Bam*H I and *Mlu* I sites.

Reporter virus MAYV-eGFP infectious clone (pACYC-MAYV-eGFP) was constructed by inserting an additional subgenomic promoter sequence (5′-GTCATACACTTGTACGGCGGTCCTAAATAGGTGCTCTACAC GACACCTATACCACC-3′) and eGFP gene into pACYC-MAYV through two rounds of overlap PCR. First, fragments covering "*Blp* I-nsP4-1stsg promoter" and "2ndsg promoter-Capsid-E2-E1-*Rsr* II" were amplified using pACYC-MAYV as template, and the "eGFP" fragment was amplified using pEGFPN1 as template. The sequences of the primers used for amplifying the specific fragments were listed in table 1 in supplemental material. The two fragments "*Blp* I-nsP4-1stsg promoter" and "eGFP" were fused together by the first step overlap PCR, generating the fragment of "*Blp* I-nsP4-1stsg promoter-eGFP". The purified product was then fused with "2ndsg promoter-Capsid-E2-E1-*Rsr* II" by the second step overlap PCR, resulting in the cassette containing "*Blp* I-nsP4-1stsg promoter-eGFP-2ndsg promoter-Capsid-E2-E1-*Rsr* II". Finally, the fragment from *Blp* I and *Rsr* II was engineered at the corresponding site into pACYC-MAYV to produce the MAYV-eGFP infectious clone. All constructs were confirmed by sequencing.

2.3. RNA transcription and transfection

The infectious clones were linearized by *Hind* III and purified by phenol/chloroform extraction. The MAYV and MAYV-eGFP RNAs were transcribed from the corresponding linearized plasmids using T7 mMEGAscript® Kit (Ambion) according to the manufacturer's protocols. Approximately 1 μg RNA was transfected into BHK-21 cells with DMRIE-C (Invitrogen). Supernatants of the transfected cells were collected at different time points after transfection, and the virus was aliquoted and stored at −80 °C for use in all experiments.

2.4. Immunofluorescence assay (IFA) and plaque assay

The RNA transfected cells were seeded on a Chamber Slide (Nalge Nunc). At different time points after transfection, the cells were fixed in cold (−20 °C) 5% acetic acid in methanol for 10 min at room temperature, washed three times with PBS and then incubated with mouse polyclonal antibody against MAYV E2 (1:200 dilution with PBS) for 1 h. After washing with PBS three times, the cells were incubated with goat anti-mouse IgG conjugated with FITC (1:125 dilution with PBS) at room temperature for 1 h. Following three times of PBS washing, the slides were mounted with 95% glycerol and analyzed under a NIKON fluorescence microscope at 400 × magnification. Virus titer and morphology were determined by single layer plaque assay with standard procedure as described previously (Deng et al., 2016).

2.5. Reverse transcription

To test the stability of the MAYV-eGFP, the reporter virus was serially passaged in BHK-21 cells for five rounds and in C6/36 cells for three rounds. For each passage, the supernatants were collected and total RNAs of the infected cells were extracted using Trizol reagent (TAKARA). Viral RNAs of each passage were amplified by one-step RT-PCR using a PrimeScript RT-PCR kit (TAKARA) with primers spanning nsP4 to Capsid gene (forward primer: 5′-ACGGAGTCGTCTCCGATAAA CTG-3′ and reverse primer: 5′-GGTTTCTTTCTACGTGGTTGCT-3′). The amplified products were analyzed by electrophoresis on 1% agarose gel.

2.6. Viral growth kinetics

Growth kinetics of MAYV and MAYV-eGFP viruses on BHK-21 and C6/36 were examined respectively. Approximately 2×10^5 BHK-21 cells and 6×10^5 C6/36 cells were seeded in a 35 mm dish. After incubation overnight, the cells were infected with 400 μL MAYV or MAYV-eGFP virus at different MOIs of 0.01, 0.05 and 0.5. After incubation for two hours, the supernatants were collected and the cells were washed with PBS for three times and replaced with fresh medium with 2% FBS. At different time points post infection, the culture medium was collected and stored at −80 °C, and subsequently subjected to plaque assay to determine the viral titer. For MAYV-eGFP infection, the expression of eGFP gene was observed under the fluorescence microscope at 100 × magnification.

2.7. Antiviral assay of MAYV-eGFP

BHK-21 cells were seeded into 96-well plates at a density of 1×10^4 cells per well. Twenty four hours later, the cells were infected with MAYV or MAYV-eGFP at an MOI of 0.05 and incubated with various concentrations of Ribavirin (0 μM–82 μM). For each drug concentration, six wells were performed in parallel. After incubation at 37 °C for 36h, the supernatants were collected and viral titers were quantified by plaque assay. For MAYV-eGFP infection, the expression of eGFP gene was observed under the fluorescence microscope at 100 × magnification, and the fluorescence value was read by Operetta imaging system (PerkinElmer). To test the antiviral activity of 6-Azauridine, 1×10^4 Vero cells were plated into 96-well plates, infected

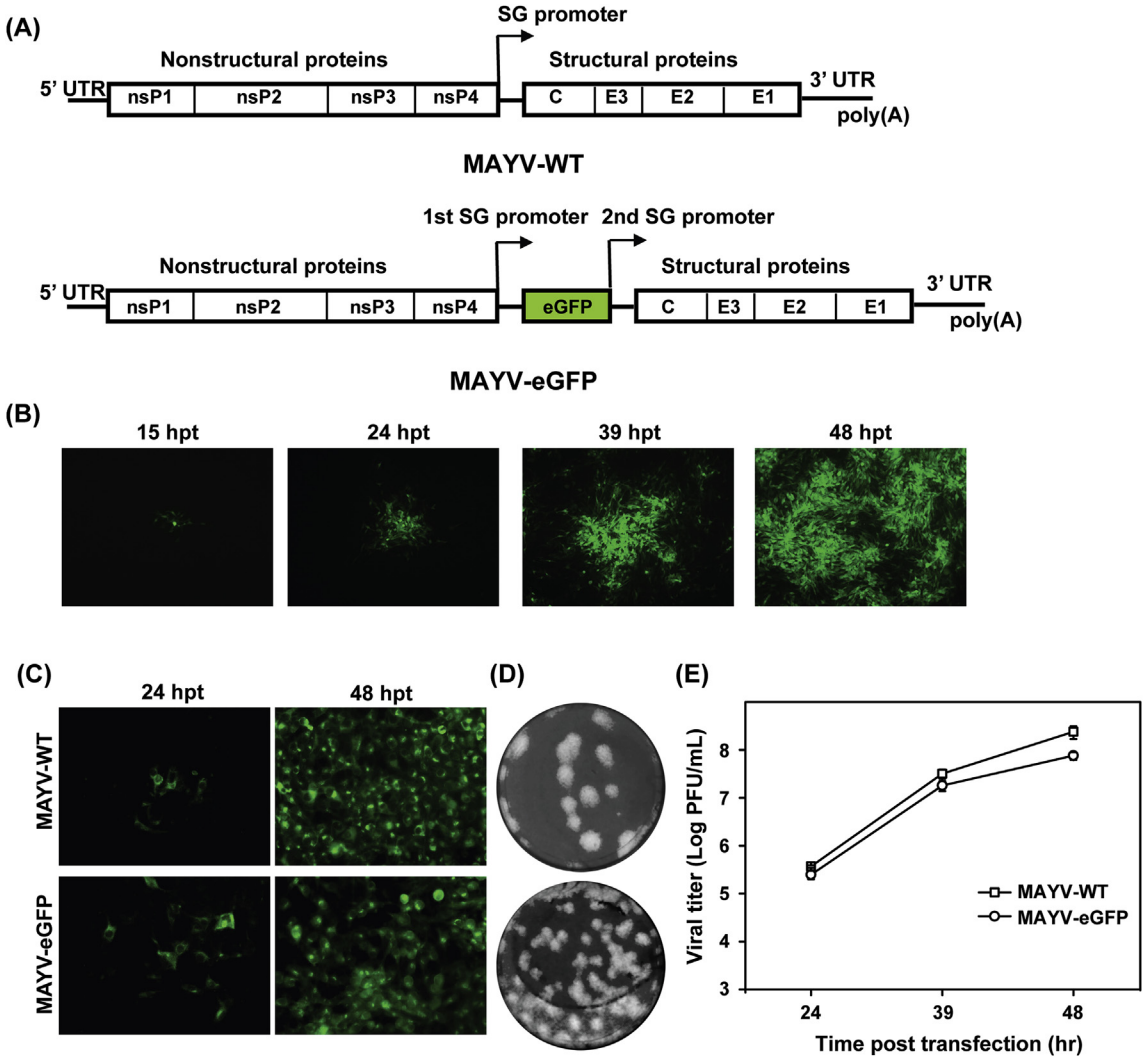

Fig. 3. Construction and characterization of MAYV-eGFP reporter virus. (A) Schematic of the recombinant MAYV-eGFP reporter virus infectious clone. An additional sg promoter and eGFP gene (shown in the green box) were inserted downstream of the 5′ORF of the pACYC-MAYV. (B) Analysis of eGFP expression in the BHK-21 cells transfected with MAYV-eGFP RNA. The BHK-21 cells were transfected with 1 μg MAYV-eGFP RNA and the expression of eGFP was detected under a fluorescent microscope at the indicated time points after transfection. (C) IFA analysis of viral protein expression in BHK-21 cells transfected with the MAYV and MAYV-eGFP RNAs respectively. (D) Plaque morphology of MAYV and MAYV-eGFP in BHK-21 cells. (E) Virus production of the supernatant of the MAYV and MAYV-eGFP RNAs transfected cells at the indicated time points post transfection. Error bars indicate the standard deviations from three independent experiments.

with MAYV-eGFP at an MOI of 0.05, and treated with different concentrations of 6-Azauridine (0 μM–20 μM). At 36 hpi, the fluorescence value was read by Operetta imaging system (PerkinElmer). The EC_{50} was calculated by nonlinear regression using Prism software (GraphPad) to determine the drug concentration required to achieve 50% of viral titer reduction or fluorescence value reduction.

3. Results

3.1. Construction and characterization of a full-length infectious clone of MAYV strain BeAr 20290

We constructed an infectious cDNA clone of the MAYV strain BeAr 20290 which was isolated from *Haemagogus* mosquitoes in 1960 in Brazil (Esposito and da Fonseca, 2015). As depicted in Fig. 1, six fragments covering the complete genome sequence of MAYV were chemically synthesized by the DNA synthesis company. In fragment A, a T7 promoter sequence was introduced upstream of the 5′UTR for further *in vitro* transcription. A poly-A tail with 34 adenosines was added downstream of the 3′UTR sequence in fragment F. The six fragments were cloned into pACYC177 or pUC19 to generate the intermediate subclones. The individual subclones were assembled step-by-step by the restriction site within the genome and vectors, resulting the infectious full-length clone pACYC-MAYV in the low-copy-number vector pACYC177 as described in materials and methods.

The MAYV RNA derived from the linearized pACYC-MAYV plasmid by *in vitro* transcription was transfected into BHK-21 cells to test the viral rescue function of the infectious clone. At different time post transfection, the cells were fixed and subjected to IFA using specific antibody against MAYV E2 protein to detect viral protein synthesis, and the supernatants were collected and subjected to plaque assay to determine the plaque morphology and virus production. As shown in Fig. 2A, IFA-positive cells were detectable at 12 hpt, and kept increasing from 12 to 48 hpt and were almost 100% among the transfected cells at 48 hpt. The cytopathic effect appeared at 24 hpt and got obvious at 48 hpt (data not shown). Accordingly, the viral titer of the supernatants showed a significant increase that reached 5×10^7 PFU/mL at 48 hpt (Fig. 2C). The viral plaque morphology measured at different time points were homogeneously large in BHK-21 cells (Fig. 2B). These results demonstrated that the virus recovered by the infectious

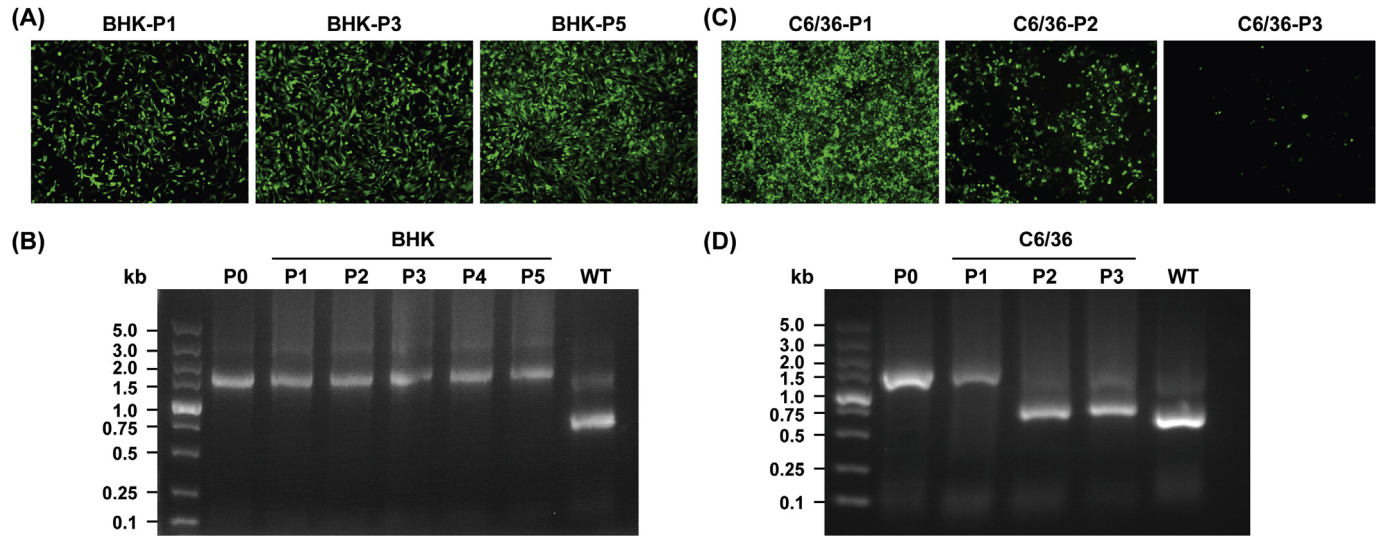

Fig. 4. Genetic stability of MAYV-eGFP in BHK-21 cells. (A) The eGFP expression of the different passages of MAYV-eGFP in BHK-21 cell. The MAYV-eGFP was serially passaged in BHK-21 cells for five rounds. Viruses from each passage (P1-P5) were used to infect 2×10^5 BHK-21 cells at an MOI of 0.1, the expression of eGFP was detected under a fluorescent microscope at 36–48h after infection. (B) Detection of the eGFP gene during virus passage in BHK-21 cell. Total RNAs from the infected cells were extracted and subjected to RT-PCR detection using the primers spanning nsP4 to Capsid gene that include the complete eGFP gene. The resulting RT-PCR products were resolved by 1% agarose gel electrophoresis. (C) The eGFP expression of the different passages of MAYV-eGFP in C6/36 cell. The MAYV-eGFP was serially passaged in C6/36 cells for three rounds. The expression of eGFP was detected under a fluorescent microscope at 96–120h after infection. (D) Detection of the eGFP gene during virus passage in C6/36 cell.

clone replicated efficiently.

3.2. Construction and characterization of the MAYV-eGFP reporter virus

After confirming the successful rescue of the recombinant MAYV, we designed the MAYV reporter virus with eGFP gene using the similar strategy used in the CHIKV-eGFP reporter virus construction previously (Deng et al., 2016). A second subgenomic promoter sequence was engineered into the pACYC-MAYV at the 5′proximal of the structural protein genes to initiate the expression of eGFP gene (Fig. 3A). The resulted clone was designated as pACYC-MAYV-eGFP as described in materials and methods. To identify whether the reporter virus could be recovered, the transcribed MAYV-eGFP RNA was transfected into BHK-21 cells, and the expression of eGFP gene was examined under a fluorescence microscope. The eGFP positive cells could be observed at 15 hpt, and quickly increased over time that almost 100% cells turned positive at 48 hpt (Fig. 3B), suggesting the high replication capacity of the reporter virus. To further compare the replication efficiency between the reporter virus and wild type (WT) virus, equal amounts of the MAYV-WT and MAYV-eGFP RNAs were transfected into BHK-21 cells. Viral protein synthesis, plaque morphology and virus production were determined by IFA and plaque assay as described above. As shown in Fig. 3D, the MAYV-eGFP displayed slightly smaller plaque morphology than that of wild type virus. However, comparable IFA positive cells and viral titers were detected for MAYV-WT and MAYV-eGFP (Fig. 3C and E) at different time points after transfection, illustrating that the insertion of the eGFP reporter gene into MAYV genome does not substantially affect viral replication in BHK-21 cell.

3.3. Stability of the MAYV-eGFP virus in cell culture

To analyze whether the eGFP reporter gene can be stably maintained in cell culture, the MAYV-eGFP virus was serially passaged in vertebrate-derived BHK-21 and mosquito-derived C6/36 cells for five and three rounds respectively. Viruses from each passage were used to infect naïve BHK-21 or C6/36 cells at an MOI of 0.1, and the percentage of cells expressing eGFP was evaluated at 36–48 hpi for BHK-21 and 96–120 hpi for C6/36 after each passage. As shown in Fig. 4A, all of the BHK-21 cells infected by P1-P5 reporter viruses showed strong fluorescence signals and nearly 100% were eGFP positive when the apparent CPE appeared, indicating the eGFP gene was stably maintained during passaging. In addition, for each passage, the RNAs of the infected cells were extracted and subjected to RT-PCR amplifying the region between nsP4 and capsid genes. Different sizes of bands were expectedly detected for WT (667 bp) and reporter virus (1460 bp) as the insertion of the eGFP gene (Fig. 4B). Each of the P1-P5 RNAs extracted from BHK-21 cells displayed a specific band showing no sequence deletion within the reporter gene which is confirmed by sequencing, further suggesting the stability of the reporter virus in BHK-21 cells. In contrast, when MAYV-eGFP was passaged in C6/36, comparable fluorescence signal was only maintained in the P1 virus infected cells, while the eGFP positive cells decreased dramatically from P2 to P3 (Fig. 4C). RT-PCR and sequencing analysis showed the eGFP gene deletion of P2 and P3 virus (Fig. 4D), confirming that the MAYV-eGFP reporter virus is not stable during passaging in C6/36 cells.

3.4. Replication kinetics of the MAYV-eGFP virus in cell culture

To develop the reporter virus based antiviral assay, we first confirmed whether the MAYV-eGFP had similar growth characteristics with wild type MAYV. Both BHK-21 and C6/36 cells were infected with MAYV-eGFP and MAYV-WT at MOIs of 0.01, 0.05 and 0.5, respectively. Viral growth kinetics were compared between the two viruses in different cells. As shown in Fig. 5A, MAYV-eGFP exhibited indistinguishable patterns of replication with wild type virus in BHK-21, whereas its viral productions were about 100-fold lower than that of wild type virus in C6/36 cells at different MOIs of infection (Fig. 5B). These results demonstrated that the MAYV-eGFP could efficiently and stably replicate in BHK-21 cell but not in C6/36 cell. BHK-21 cell was chosen for the optimization of viral infection for antiviral assay. We further identified the proper infection MOI value and the time point for detection by monitoring the eGFP positive cells at different time after infection with MAYV-eGFP at varied MOIs. The eGFP positive cells increased in a dose- and time-dependent manner (Fig. 5C), illustrating that the eGFP signal correlated well with the reporter virus replication. Almost 100% cells displayed strong eGFP signal when the cells were

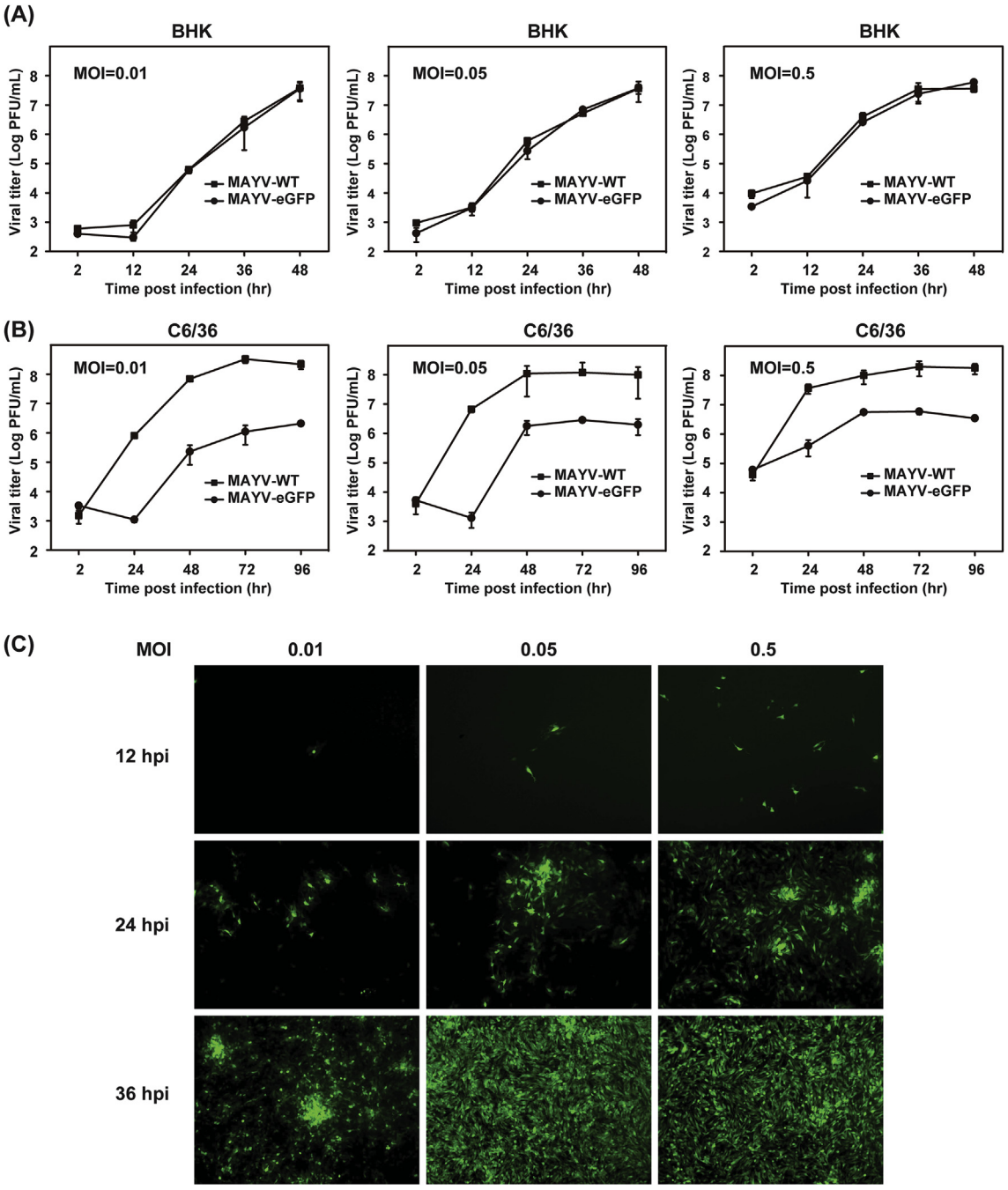

Fig. 5. Optimization of the MAYV-eGFP infection for antiviral assay. (A) Growth kinetics of the wild type MAYV and MAYV-eGFP on BHK cells at MOIs of 0.01, 0.05 and 0.5. (B) Growth kinetics of the wild type MAYV and MAYV-eGFP on C6/36 cells at MOIs of 0.01, 0.05 and 0.5. Error bars indicate the standard deviations from three independent experiments. (C) The eGFP expression of the BHK-21 cells infected with MAYV-eGFP at MOIs of 0.01, 0.05 and 0.5 respectively. The eGFP gene expression was detected under a fluorescent microscope at the indicated time points after infection.

infected by MAYV-eGFP at an MOI of 0.05 at 36 hpi. Therefore, we determined the infection MOI of 0.05, eGFP observation at 36 hpi and BHK-21 cell type as the infection condition for the following antiviral assay.

3.5. Antiviral activity evaluation based on the MAYV-eGFP reporter virus

Ribavirin was a broad-spectrum antiviral drug and had been reported to have inhibitory effect on alphavirus replication (Coffey et al., 2011; Markland et al., 2000). In order to validate the utility of MAYV-eGFP reporter virus for antiviral screening, we compared the antiviral ability of ribavirin on MAYV-eGFP and MAYV-WT viruses. BHK-21 cells were infected with MAYV-eGFP and MAYV-WT respectively at an MOI of 0.05 and treated with different concentrations of ribavirin (0 μM-82 μM) at the same time. At 36 hpi, the eGFP gene expression was detected under a fluorescence microscope, the fluorescence value was read by Operetta imaging system (PerkinElmer) and viral titers were determined by plaque assay. The amount of eGFP positive cells and fluorescence value in the MAYV-eGFP infected BHK-21 decreased dramatically in a dose-dependent manner of ribavirin (Fig. 6A and D). The EC_{50} of ribavirin calculated by fluorescence value reduction was 2.35 μM. Consistently, viral titers of the supernatants from both MAYV-eGFP and MAYV-WT infected cells reduced with the increase of ribavirin concentration (Fig. 6B and C). The EC_{50} of ribavirin calculated by

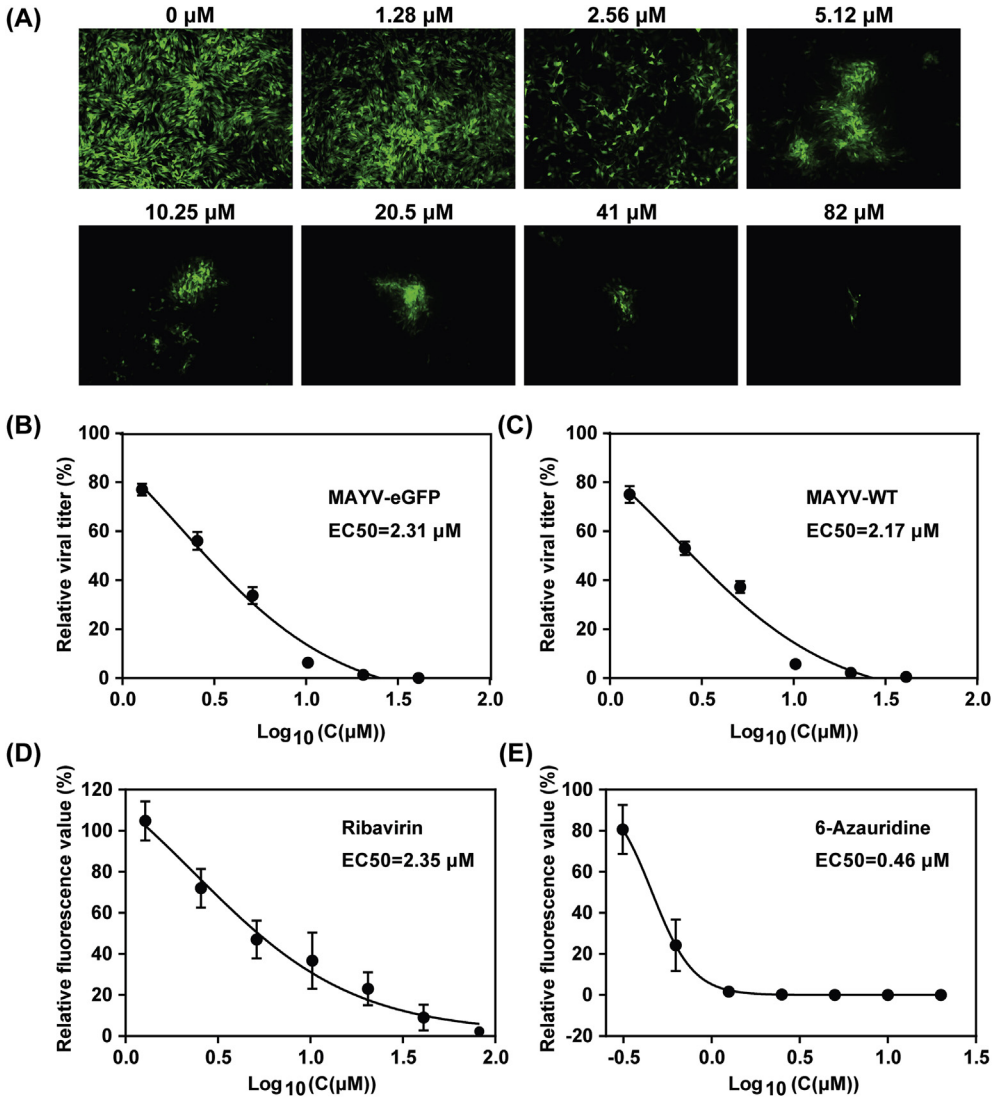

Fig. 6. Antiviral activity of ribavirin on wild type MAYV and MAYV-eGFP. (A) Effects of different concentrations of ribavirin on the eGFP expression of the MAYV-eGFP infected cells. BHK-21 cells were infected with MAYV-eGFP at an MOI of 0.05 and incubated with the indicated concentrations of ribavirin, the eGFP gene expression was detected under a fluorescent microscope at 36 hpi. (B) Viral titer reduction of MAYV-eGFP with the treatment of different concentrations of ribavirin. Supernatants of the MAYV-eGFP infected cells were collected at 36 hpi, and viral titers were determined by plaque assay. (C) Viral titer reduction of wild type MAYV with the treatment of different concentrations of ribavirin. Supernatants of the MAYV infected cells were collected at 36 hpi, and viral titers were determined by plaque assay. (D) Fluorescence value reduction of MAYV-eGFP infected BHK-21 cells treated with the treatment of different concentrations of ribavirin. The fluorescence values of the cells were read by Operetta imaging system (PerkinElmer) at 36 hpi. (E) Fluorescence value reduction of MAYV-eGFP with the treatment of different concentrations of 6-Azauridine. Vero cells were infected with MAYV-eGFP at an MOI of 0.05, and incubated with the indicated concentrations of 6-Azauridine. Fluorescence values were read at 36 hpi, EC_{50} were calculated by nonlinear regression using Prism software (GraphPad). Error bars indicate the standard deviations from three independent experiments.

viral titer reduction efficiency were 2.31 μM for MAYV-eGFP and 2.17 μM for MAYV-WT respectively. These results indicated that the anti-MAYV activity of compound can be rapidly evaluated by eGFP signal detection of the MAYV-eGFP infected cells. We further tested the antiviral activity against MAYV of 6-Azauridine, a compound which was more effective against CHIKV and SFV compared to ribavirin (Briolant et al., 2004). Vero cells were infected with MAYV-eGFP at an MOI of 0.05 and treated with various concentrations of 6-Azauridine (0 μM–20 μM). The fluorescence value was read at 36 hpi. As depicted in Fig. 6F and 6-Azauridine showed a significant inhibitory effect on MAYV-eGFP replication with a EC_{50} of 0.46 μM, which was lower than the reported inhibitory concentration of CHIKV and SFV (0.82 μM and 1.6 μM, respectively) (Briolant et al., 2004). Overall, these results demonstrated that the MAYV-eGFP reporter virus provides a rapid and precise tool for antiviral inhibitors screening against MAYV.

4. Discussion

In recent years, arboviruses including WNV, DENV, ZIKV and CHIKV had re-emerged and caused several worldwide outbreaks (Hotez and Murray, 2017). As a mosquito-borne virus that threatens human health, MAYV is typically neglected that there are few studies of this important pathogen in the existing literatures (Hotez and Murray, 2017). In order to develop reliable tools for MAYV study, in this study, we successfully constructed the infectious clones of MAYV and an eGFP reporter virus. By the standard virus rescue procedure, we identified that the MAYV-eGFP virus showed indistinguishable high replication efficiency with the wild type MAYV in BHK-21 cells. The eGFP gene expression level within the MAYV-eGFP infected cells correlated well with the viral replication, inferring that the growth of reporter virus can be monitored directly by eGFP observation. After validating the good stability of the reporter virus in BHK-21, we confirmed the feasibility of the MAYV-eGFP for rapid antiviral screening assay using the known inhibitor ribavirin and 6-Azauridine.

Reverse genetic system is powerful molecular tool for the study of RNA viruses. Infectious cDNA clones have been obtained for several familiar alphaviruses, such as CHIKV, SINV, SFV, VEEV and RRV. As for MAYV, only a full-length infectious clone of MAYV strain CH which was isolated from human patient in Peru in 2001 was reported by William J. Weise and coworkers (Weise et al., 2014). Here, we generated the infectious clone of the MAYV strain BeAr 20290 which was isolated from *Haemagogus* mosquitoes in 1960 in Brazil (Esposito and da Fonseca, 2015). Previous phylogenetic study showed high genetic divergence between different MAYV genotypes with potential geographical and temporal range (Auguste et al., 2015), therefore, constructions of the infectious clones of different viral strains would be helpful for evolutionary and ecological analyses of MAYV.

One of the common strategies used for the reporter alphaviruses construction is to express the reporter gene by introducing a second copy of subgenomic promoter into viral genome. Previous studies have

identified that the sg promoter and the heterologous gene sequences inserted downstream of the 5′ORF is more stable than being placed downstream of the 3′ORF within the Sindbis virus genome (Pierro et al., 2003; Pugachev et al., 1995). Consistent with their results, by engineering the sg promoter and eGFP gene downstream of the 5′ORF, both the CHIKV-eGFP which we had constructed previously (Deng et al., 2016) and MAYV-eGFP in this work showed great stability that can be stably maintained for at least five rounds' passages in BHK-21 cells. The insertion of reporter genes into viral genome have been reported to attenuate virus replication to different extends. The SFV-eGFP reporter virus showed a slower replication kinetic than the parental virus in BHK-21 cells (Tamberg et al., 2007). The viral production of CHIKV-eGFP reporter virus was also 10-fold lower than that of wild type CHIKV in BHK-21 (Deng et al., 2016). However, we had identified that the MAYV-eGFP reporter virus replicated as efficiently as the MAYV-WT in BHK-21 (Figs. 3E and 5A), but exhibited reduced replication efficacy in comparison with the MAYV-WT in C6/36 cells (Fig. 5B). Moreover, the eGFP gene can be stably maintained in BHK-21 cells but not in C6/36 cells (Fig. 4). We supposed the possible explanation for this phenomenon is that the insertion of an additional ORF into the viral genome may affect RNA replication and the stability of inserted gene in C6/36 but not in BHK-21 cells. Further work is needed to test this hypothesis.

Among alphaviruses, a few high throughput-screening systems have been developed for CHIKV antiviral discovery. A CHIKV 26S subgenomic RNA encoding the structural proteins based HTS was established to screen the virus fusion inhibitors (Wang et al., 2016). Megha Aggarwal and coworkers have adopted a fluorescence resonance energy transfer (FRET) based proteolytic assay for HTS to identify the serine protease inhibitor of CHIKV capsid protein (Aggarwal et al., 2015). Besides, a fluorescence polarization based HTS assay was developed for screening small molecules against the CHIKV nsP1 capping enzyme (Bullard-Feibelman et al., 2016). These systems only target the specific steps during viral life cycle that cannot screen for inhibitors aiming to the complete replication cycle. So far, the antiviral screening approaches for MAYV still rely on the traditional viral RNA quantification, the CPE evaluation and plaque reduction assays that are time-consuming and labor-intensive. Here, we described the MAYV-eGFP reporter virus based antiviral assay capable of evaluating the antiviral activity by direct eGFP signal detection. Comparing with the traditional methods, this assay shortens the time needed to conduct the antiviral screening, and most importantly, it allows for screening of antiviral compounds targeting the whole viral life cycle. In addition, the fluorescent image based high-content screening (HCS) assay had been developed for several reporter viruses (Cook et al., 2018) or subgenomic replicons (Hao and Duggal, 2009). The HCS assay completed by automated high-speed and high-resolution microscopy can analyze the antiviral efficiency with the fluorescent images in a quantitative and high throughput manner. The MAYV-eGFP also can be established for HCS assay to identify inhibitors from large compound libraries for primary screening in the future studies.

In summary, we have established the reverse genetic system for MAYV. The MAYV-eGFP reporter virus showed good stability and efficient replication as the wild type virus in BHK-21 cell. The reporter virus based antiviral assay developed in this study will facilitate the antiviral screening for novel anti-MAYV agents.

Acknowledgements

We thank the Core Facility and Technical Support, Wuhan Institute of Virology and Wuhan Key Laboratory on Emerging Infectious Diseases and Biosafety for helpful supports during the course of the work. This work was supported by the National Key Research and Development Program of China (2018YFA0507201), the Key Research Program of the Chinese Academy of Sciences(ZDRW-ZS-2016-4-2), the National Natural Science Foundation of China(81572003).

Appendix A. Supplementary data

Supplementary data to this article can be found online at https://doi.org/10.1016/j.antiviral.2019.05.013.

References

Acosta-Ampudia, Y., Monsalve, D.M., Rodriguez, Y., Pacheco, Y., Anaya, J.M., Ramirez-Santana, C., 2018. Mayaro: an emerging viral threat? Emerg. Microb. Infect. 7, 163.
Aggarwal, M., Sharma, R., Kumar, P., Parida, M., Tomar, S., 2015. Kinetic characterization of trans-proteolytic activity of Chikungunya virus capsid protease and development of a FRET-based HTS assay. Sci. Rep. 5, 14753.
Amorim, R., de Meneses, M.D.F., Borges, J.C., da Silva Pinheiro, L.C., Caldas, L.A., Cirne-Santos, C.C., de Mello, M.V.P., de Souza, A.M.T., Castro, H.C., de Palmer Paixao, I.C.N., Campos, R.M., Bergmann, I.E., Malirat, V., Bernardino, A.M.R., Rebello, M.A., Ferreira, D.F., 2017. Thieno[2,3-b]pyridine derivatives: a new class of antiviral drugs against Mayaro virus. Arch. Virol. 162, 1577–1587.
Anderson, C.R., Downs, W.G., Wattley, G.H., Ahin, N.W., Reese, A.A., 1957. Mayaro virus: a new human disease agent. II. Isolation from blood of patients in Trinidad. B.W.I. Am. J. Trop. Med. Hyg. 6, 1012–1016.
Auguste, A.J., Liria, J., Forrester, N.L., Giambalvo, D., Moncada, M., Long, K.C., Morón, D., de Manzione, N., Tesh, R.B., Halsey, E.S., Kochel, T.J., Hernandez, R., Navarro, J.C., Weaver, S.C., 2015. Evolutionary and ecological characterization of mayaro virus strains isolated during an outbreak, Venezuela, 2010. Emerg. Infect. Dis. 21, 1742–1750.
Briolant, S., Garin, D., Scaramozzino, N., Jouan, A., Crance, J.M., 2004. In vitro inhibition of Chikungunya and Semliki Forest viruses replication by antiviral compounds: synergistic effect of interferon-alpha and ribavirin combination. Antivir. Res. 61, 111–117.
Brunini, S., Franca, D.D.S., Silva, J.B., Silva, L.N., Silva, F.P.A., Spadoni, M., Rezza, G., 2017. High frequency of mayaro virus IgM among febrile patients, Central Brazil. Emerg. Infect. Dis. 23, 1025–1026.
Bullard-Feibelman, K.M., Fuller, B.P., Geiss, B.J., 2016. A sensitive and robust high-throughput screening assay for inhibitors of the chikungunya virus nsP1 capping enzyme. PLoS One 11, e0158923.
Caldas, L.A., Ferreira, D.F., Freitas, T.R.P., 2018. Prostaglandin A1 triggers Mayaro virus inhibition and heat shock protein 70 expression in an epithelial cell model. Rev. Soc. Bras. Med. Trop. 51, 584–590.
Camini, F.C., da Silva, T.F., da Silva Caetano, C.C., Almeida, L.T., Ferraz, A.C., Alves Vitoreti, V.M., de Mello Silva, B., de Queiroz Silva, S., de Magalhaes, J.C., de Brito Magalhaes, C.L., 2018. Antiviral activity of silymarin against Mayaro virus and protective effect in virus-induced oxidative stress. Antivir. Res. 158, 8–12.
Carvalho, C.A., Sousa Jr., I.P., Silva, J.L., Oliveira, A.C., Goncalves, R.B., Gomes, A.M., 2014. Inhibition of Mayaro virus infection by bovine lactoferrin. Virology 452–453, 297–302.
Coffey, L.L., Beeharry, Y., Borderia, A.V., Blanc, H., Vignuzzi, M., 2011. Arbovirus high fidelity variant loses fitness in mosquitoes and mice. Proc. Natl. Acad. Sci. U. S. A. 108, 16038–16043.
Cook, E., Hermes, J., Li, J., Tudor, M., 2018. High-content reporter assays. Methods Mol. Biol. 1755, 179–195.
de Thoisy, B., Gardon, J., Salas, R.A., Morvan, J., Kazanji, M., 2003. Mayaro virus in wild mammals, French Guiana. Emerg. Infect. Dis. 9, 1326–1329.
Deng, C.L., Liu, S.Q., Zhou, D.G., Xu, L.L., Li, X.D., Zhang, P.T., Li, P.H., Ye, H.Q., Wei, H.P., Yuan, Z.M., Qin, C.F., Zhang, B., 2016. Development of neutralization assay using an eGFP chikungunya virus. Viruses 8.
Esposito, D.L., da Fonseca, B.A., 2015. Complete Genome Sequence of Mayaro Virus (Togaviridae, Alphavirus) Strain BeAr 20290 from Brazil. Genome Announc 3.
Firth, A.E., Chung, B.Y., Fleeton, M.N., Atkins, J.F., 2008. Discovery of frameshifting in Alphavirus 6K resolves a 20-year enigma. Virol. J. 5, 108.
Friedrich-Janicke, B., Emmerich, P., Tappe, D., Gunther, S., Cadar, D., Schmidt-Chanasit, J., 2014. Genome analysis of Mayaro virus imported to Germany from French Guiana. Emerg. Infect. Dis. 20, 1255–1257.
Hao, W., Duggal, R., 2009. High-throughput screening of HCV RNA replication inhibitors by means of a reporter replicon system. Methods Mol. Biol. 510, 243–250.
Henrik Gad, H., Paulous, S., Belarbi, E., Diancourt, L., Drosten, C., Kummerer, B.M., Plate, A.E., Caro, V., Despres, P., 2012. The E2-E166K substitution restores Chikungunya virus growth in OAS3 expressing cells by acting on viral entry. Virology 434, 27–37.
Hotez, P.J., Murray, K.O., 2017. Dengue, west nile virus, chikungunya, Zika-and now mayaro? PLoS Negl. Trop. Dis. 11, e0005462.
Kummerer, B.M., Grywna, K., Glasker, S., Wieseler, J., Drosten, C., 2012. Construction of an infectious Chikungunya virus cDNA clone and stable insertion of mCherry reporter genes at two different sites. J. Gen. Virol. 93, 1991–1995.
Lednicky, J., De Rochars, V.M., Elbadry, M., Loeb, J., Telisma, T., Chavannes, S., Anilis, G., Cella, E., Ciccozzi, M., Okech, B., Salemi, M., Morris Jr., J.G., 2016. Mayaro virus in child with acute febrile illness, Haiti, 2015. Emerg. Infect. Dis. 22, 2000–2002.
LeDuc, J.W., Pinheiro, F.P., Travassos da Rosa, A.P., 1981. An outbreak of Mayaro virus disease in Belterra, Brazil. II. Epidemiology. Am. J. Trop. Med. Hyg. 30, 682–688.
Long, K.C., Ziegler, S.A., Thangamani, S., Hausser, N.L., Kochel, T.J., Higgs, S., Tesh, R.B., 2011. Experimental transmission of Mayaro virus by Aedes aegypti. Am. J. Trop. Med. Hyg. 85, 750–757.
Markland, W., McQuaid, T.J., Jain, J., Kwong, A.D., 2000. Broad-spectrum antiviral activity of the IMP dehydrogenase inhibitor VX-497: a comparison with ribavirin and demonstration of antiviral additivity with alpha interferon. Antimicrob. Agents Chemother. 44, 859–866.

Mourao, M.P., Bastos Mde, S., de Figueiredo, R.P., Gimaque, J.B., Galusso Edos, S., Kramer, V.M., de Oliveira, C.M., Naveca, F.G., Figueiredo, L.T., 2012. Mayaro fever in the city of Manaus, Brazil, 2007-2008. Vector Borne Zoonotic Dis. 12, 42–46.
Neumayr, A., Gabriel, M., Fritz, J., Gunther, S., Hatz, C., Schmidt-Chanasit, J., Blum, J., 2012. Mayaro virus infection in traveler returning from Amazon Basin, northern Peru. Emerg. Infect. Dis. 18, 695–696.
Phillips, A.T., Rico, A.B., Stauft, C.B., Hammond, S.L., Aboellail, T.A., Tjalkens, R.B., Olson, K.E., 2016. Entry sites of Venezuelan and western equine encephalitis viruses in the mouse central nervous system following peripheral infection. J. Virol. 90, 5785–5796.
Pierro, D.J., Myles, K.M., Foy, B.D., Beaty, B.J., Olson, K.E., 2003. Development of an orally infectious Sindbis virus transducing system that efficiently disseminates and expresses green fluorescent protein in Aedes aegypti. Insect Mol. Biol. 12, 107–116.
Pugachev, K.V., Mason, P.W., Shope, R.E., Frey, T.K., 1995. Double-subgenomic Sindbis virus recombinants expressing immunogenic proteins of Japanese encephalitis virus induce significant protection in mice against lethal JEV infection. Virology 212, 587–594.
Ralambondrainy, M., Belarbi, E., Viranaicken, W., Baranauskiene, R., Venskutonis, P.R., Despres, P., Roques, P., El Kalamouni, C., Selambarom, J., 2018. In vitro comparison of three common essential oils mosquito repellents as inhibitors of the Ross River virus. PLoS One 13, e0196757.
Shang, B., Deng, C., Ye, H., Xu, W., Yuan, Z., Shi, P.Y., Zhang, B., 2013. Development and characterization of a stable eGFP enterovirus 71 for antiviral screening. Antivir. Res. 97, 198–205.
Strauss, J.H., Strauss, E.G., 1994. The alphaviruses: gene expression, replication, and evolution. Microbiol. Rev. 58, 491–562.
Sun, C., Gardner, C.L., Watson, A.M., Ryman, K.D., Klimstra, W.B., 2014. Stable, high-level expression of reporter proteins from improved alphavirus expression vectors to track replication and dissemination during encephalitic and arthritogenic disease. J. Virol. 88, 2035–2046.
Tamberg, N., Lulla, V., Fragkoudis, R., Lulla, A., Fazakerley, J.K., Merits, A., 2007. Insertion of EGFP into the replicase gene of Semliki Forest virus results in a novel, genetically stable marker virus. J. Gen. Virol. 88, 1225–1230.
Taylor, S.F., Patel, P.R., Herold, T.J., 2005. Recurrent arthralgias in a patient with previous Mayaro fever infection. South. Med. J. 98, 484–485.
Vanlandingham, D.L., Tsetsarkin, K., Hong, C., Klingler, K., McElroy, K.L., Lehane, M.J., Higgs, S., 2005. Development and characterization of a double subgenomic chikungunya virus infectious clone to express heterologous genes in Aedes aegypti mosquitoes. Insect Biochem. Mol. Biol. 35, 1162–1170.
Wang, Y.M., Lu, J.W., Lin, C.C., Chin, Y.F., Wu, T.Y., Lin, L.I., Lai, Z.Z., Kuo, S.C., Ho, Y.J., 2016. Antiviral activities of niclosamide and nitazoxanide against chikungunya virus entry and transmission. Antivir. Res. 135, 81–90.
Weise, W.J., Hermance, M.E., Forrester, N., Adams, A.P., Langsjoen, R., Gorchakov, R., Wang, E., Alcorn, M.D., Tsetsarkin, K., Weaver, S.C., 2014. A novel live-attenuated vaccine candidate for mayaro Fever. PLoS Negl. Trop. Dis. 8, e2969.
Weisshaar, M., Cox, R., Morehouse, Z., Kumar Kyasa, S., Yan, D., Oberacker, P., Mao, S., Golden, J.E., Lowen, A.C., Natchus, M.G., Plemper, R.K., 2016. Identification and characterization of influenza virus entry inhibitors through dual myxovirus high-throughput screening. J. Virol. 90, 7368–7387.
Zhang, Z., Yang, E., Hu, C., Cheng, H., Chen, C.Y., Huang, D., Wang, R., Zhao, Y., Rong, L., Vignuzzi, M., Shen, H., Shen, L., Chen, Z.W., 2017. Cell-based high-throughput screening assay identifies 2',2'-Difluoro-2'-deoxycytidine gemcitabine as a potential antipoliovirus agent. ACS Infect. Dis. 3, 45–53.
Zou, G., Xu, H.Y., Qing, M., Wang, Q.Y., Shi, P.Y., 2011. Development and characterization of a stable luciferase dengue virus for high-throughput screening. Antivir. Res. 91, 11–19.